Non-uniform k-Connectivity for Energy-Efficient and Reliable Underwater Wireless Sensor Networks

Cagla Tantur Karagul
Electr. & Electron. Eng.
TOBB Univ. of Econ. & Tech.
Ankara, Turkey
ckaragul@etu.edu.tr

Mehmet Burak Akgun
Computer Eng.
TOBB Univ. of Econ. & Tech.
Ankara, Turkey
m.akgun@etu.edu.tr

Huseyin Ugur Yildiz
Electr. & Electron. Eng.
TED University
Ankara, Turkey
hugur.yildiz@tedu.edu.tr

Bulent Tavli
Electr. & Electron. Eng.
TOBB Univ. of Econ. & Tech.
Ankara, Turkey
btavli@etu.edu.tr

***Abstract*—Underwater wireless sensor networks (UWSNs) have diverse applications, including coastal monitoring, environmental observation, and defense operations. Resilient underwater missions require reliable connectivity, often realized through k-connectivity, where each sensor node sustains at least k disjoint paths to the base station (BS). However, maintaining k paths for every node introduces substantial energy overhead, limiting network lifetime. To address this challenge, we propose a *non-uniform k-connectivity* scheme, assigning higher k values to critical nodes and lower ones to less critical nodes, for reducing the total energy consumption. We formulate this approach as a mixed-integer linear programming (MILP) model and evaluate it on a coastal UWSN scenario. Our results show that overall energy consumption can increase up to 6.17-fold in a fully 3-connected network compared to the 1-connected case, whereas *non-uniform k-connectivity* can reduce this overhead to 4.16-fold, achieving a more balanced trade-off between reliability and energy efficiency.**

***Index Terms*—underwater wireless sensor networks, k-connectivity, reliability, energy efficiency, mixed-integer linear programming.**

I. Introduction

Although more than seventy percent of the Earth's surface is covered with water, our knowledge of the oceans is still limited, driving a great interest in underwater research for applications such as coastal monitoring, pollution control, climate studies, and defense missions [1]. A commonly used technology for effectively monitoring the underwater environment is underwater wireless sensor networks (UWSNs). A typical UWSN consists of numerous battery-limited sensor nodes deployed on or above the seabed with the ability to sense, collect, and transmit data via acoustic communication, together with a central base station (BS) floating on the water's surface that aggregates the collected data [2].

For UWSNs to operate reliably over long periods of time, both efficient battery power management and maintaining reliable routing paths are essential [3]. Since sensor nodes are usually placed in hard-to-reach locations, replacing their batteries is impractical. Hence, it is critical that the nodes consume their energy in an optimized manner to prolong the network lifetime. At the same time, harsh conditions of the underwater acoustic channel disrupt routing paths. Therefore, enhancing the network reliability is just as important as achieving the energy efficiency of the network.

A common method used for improving the network reliability in wireless sensor networks (WSNs) is k-connectivity [4]. Unlike its classic definition, where each node must have at least k paths to all other nodes, in this work, we define k-connectivity as each sensor node in the network having at least k node-disjoint paths (i.e., paths that do not share intermediate nodes) to the BS, which better reflects the convergecast data-collection nature of UWSNs.

There are very few studies in WSNs literature that evaluate network lifetime and k-connectivity interaction. [5] addresses the balance between network lifetime and reliability in terms of k-connectivity for *terrestrial* WSNs. The results shows that maximizing network lifetime reduces k-connectivity by 20%, while maximizing k-connectivity reduces network lifetime by 35%. In contrast, [6] analyzes the lifetime–reliability trade-off for underwater WSNs. This study shows that maintaining 5-connectivity in UWSNs reduces network lifetime by over 33%. It is important to note that both studies primarily focus on *uniform* k-connectivity, where every node is connected to the BS by at least k node-disjoint paths.

In many underwater applications, using a uniform reliability level for all nodes is unnecessary. Critical nodes that monitor sensitive areas or carry high-priority traffic require higher k values, while other nodes can operate at lower connection levels without compromising general task objectives. In this way, the *non-uniform k-connectivity* approach, which assigns different k values to nodes based on their roles, has the potential to reduce overall reliability costs and extend network lifetime.

In many underwater applications, using a uniform reliability level for all nodes is unnecessary. Critical nodes monitoring sensitive areas or carrying priority traffic require higher k values, while others can operate with lower connectivity without affecting mission goals. This *non-uniform k-connectivity* approach assigns different k values based on node roles, reducing overall reliability costs and extending network lifetime.

To the best of our knowledge, the concept of *non-uniform k-connectivity*, with the analysis on a coastal UWSN, has not been previously studied in the literature. To address this gap, in this work, we defined our network model for a coastal UWSN model and developed a mixed-integer linear programming (MILP) model that facilitates *non-uniform* k assignments per

node, explicitly accounting for for both data and control packet energy costs in maintaining node-disjoint paths to the BS. Using the optimal solutions of the MILP model, we address the trade-off between network reliability and lifetime in UWSNs with the analysis on a coastal UWSN model.

II. System Model

The UWSN is modeled as a 2D shallow-water linear topology tailored to a coastal application. 12 stationary sensor nodes are anchored on the seabed at a depth of 20 m and are evenly distributed along the x-axis across a 3 km span, from node-1 at $x = 0$ km to node-12 at $x = 3$ km. Two BS deployment scenarios are investigated: in the first, the BS is placed at the shoreline at $x = 0$ km on the water surface, while in the second, the BS is located at the midpoint of the network at $x = 1.5$ km. The network topology is shown in Fig. 1a.

The network topology is modeled as a directed graph $\mathcal{G} = (\mathcal{V}, \mathcal{A})$, where $\mathcal{V}$ is the set of all nodes (including the BS) and $\mathcal{A} = \{(i,j) : i \in \mathcal{V},\ j \in \mathcal{V} \setminus \{i\},\ d_{ij} \leq \mathcal{R}_{\max}(\ell_{\max})\}$ is the set of feasible communication links, where d_{ij} denotes the Euclidean distance between nodes-i and j. $\mathcal{W}$ represents the set of all sensor nodes (excluding the BS). Link feasibility is determined by the maximum transmission range $\mathcal{R}_{\max}(\ell)$, which depends on the transmission power level-ℓ. Ten discrete transmission power levels are defined as $\mathcal{P} = \{1, 2, \ldots, 10\}$, where $\ell_{\max} = 10$ corresponds to the highest power level, and each transmitter selects the minimum $\ell \in \mathcal{P}$ required to reach the intended receiver. The corresponding transmission energy costs and ranges for each power level are given in Table I. We also define $\mathcal{L} = \{1, \ldots, \eta_l\}$ as the set of path indices, where $\eta_l = 5$ is the maximum number of paths for each source node. We also define $\mathcal{L} = \{1, \ldots, \eta_l\}$ as the set of path indices, where $\eta_l = 5$ is the maximum number of paths for each node.

TABLE I: Energy cost for transmission ($\mathcal{E}_{\mathrm{T}}(\ell)$ – mJ/bit) and the communication distance ($\mathcal{R}_{\max}(\ell)$ – m) at power level-ℓ.

ℓ	$\mathcal{E}_{\mathrm{T}}(\ell)$	$\mathcal{R}_{\max}(\ell)$	ℓ	$\mathcal{E}_{\mathrm{T}}(\ell)$	$\mathcal{R}_{\max}(\ell)$
1	0.115	100	6	3.416	600
2	0.375	200	7	4.954	700
3	0.792	300	8	6.967	800
4	1.404	400	9	9.568	900
5	2.258	500	10	12.897	1000

The network operates for $\mathcal{N}_\tau = 1440$ rounds, each lasting $\tau = 300$ s. In every round, each sensor node-k generates $Q_k = 1$ data packet of size $L_{\mathrm{pkt}} = 1024$ bits. Additionally, control packets of size $L_{\mathrm{cnt}} = 256$ bits are sent over each active link at a relative frequency ψ with respect to data generation, and these packets are used for link maintenance. The data rate is $\lambda_{\mathrm{data}} = 2500$ bps. Both single-hop and multi-hop routes to the BS are permitted. Each sensor node maintains at least κ_n node-disjoint paths to the BS.

The energy model follows the acoustic communication framework in [7]. Transmission loss at range $\mathcal{R}_{\max}(\ell)$ is computed using a spreading factor of $k_s = 1.5$ and the absorption coefficient

$$\alpha(f_0) = \frac{0.11 f_0^2}{1 + f_0^2} + \frac{44 f_0^2}{4100 + f_0^2} + 2.75 \times 10^{-4} f_0^2 + 0.003, \quad (1)$$

derived from Thorp's formula for $f_0 = 25$ kHz. The transmission loss is then given by

$$\Lambda(\mathcal{R}_{\max}(\ell)) = \mathcal{R}_{\max}(\ell)^{k_s} \times \nu^{10^{-3}\mathcal{R}_{\max}(\ell)}, \quad (2)$$

where $\nu = 10^{0.1\alpha(f_0)}$. The transmission energy per bit using power level-ℓ is obtained by multiplying the transmission loss with the target receive power $P_0 = 1\times$ 10^{-7} J/bit as $\mathcal{E}_{\mathrm{T}}(\ell) = \Lambda(\mathcal{R}_{\max}(\ell)) \times P_0$, while the reception cost is a constant: $\mathcal{E}_{\mathrm{R}} =$ 0.2 $\times$ 10^{-7} J/bit. Each node selects the minimum transmission energy level that can cover the link distance d_{ij}. If d_{ij} is within the range of the lowest power level (i.e., $\ell = 1$), that level is chosen; if it exceeds the maximum range of the highest level, the link is considered infeasible; otherwise, the next higher level whose range just exceeds d_{ij} is selected. We use $\mathcal{E}^*_{\mathrm{T},ij}$ to denote the transmission energy per bit corresponding to the selected level for the link from node i to node j. The MILP model aims to maximize network lifetime under *non-uniform k-connectivity* requirement. The objective is to minimize the energy dissipation of the most energy-demanding node (i.e., $\mathcal{E}_{\max}$) [8], [9]:

$$\text{Minimize } \mathcal{E}_{\max}. \quad (3)$$

The proposed MILP model incorporates the constraints given in (4)–(15). Constraint (4) enforces data conservation for each node according to its role in the network (source: $i = k$, BS: $i = 1$, or relay). In this constraint, u_{ij}^{kl} represents the number of data packets transmitted from node-i to node-j on the l-th path originating from source node-k. z_k^l denotes the number of data packets injected tthe networkrk on the l-th path by source node-k. The total number of data packets generated bthe sourcece node-k during the operational lifetime of the UWSN is computed as $\sum_{l=1}^{\eta_l} z_k^l = Q_k \times \mathcal{N}_\tau,\ \forall k \in \mathcal{W}$.

$$\sum_{(i,j)\in\mathcal{A}} u_{ij}^{kl} - \sum_{(j,i)\in\mathcal{A}} u_{ji}^{kl} = \begin{cases} z_k^l, & \text{if } i = k, \\ -z_k^l, & \text{if } i = 1, \\ 0, & \text{otherwise}, \end{cases} \quad \forall i \in \mathcal{V},\ k \in \mathcal{W},\ l \in \mathcal{L} \quad (4)$$

Constraint (5) prevents the data from returning to its originating source node.

$$\sum_{l=1}^{\eta_l} \sum_{j\in\mathcal{W}} u_{jk}^{kl} = 0, \quad \forall k \in \mathcal{W} \quad (5)$$

Constraint (6) ensures that the total flow u_{ij}^{kl} on each link remains bounded by the maximum data generated ($Q_k \times \mathcal{N}\tau$), which is governed by the binary path selection variable n_{ij}^{kl}. Moreover, this constraint enforces the reverse relation, preventing a path from being considered active unless there is a

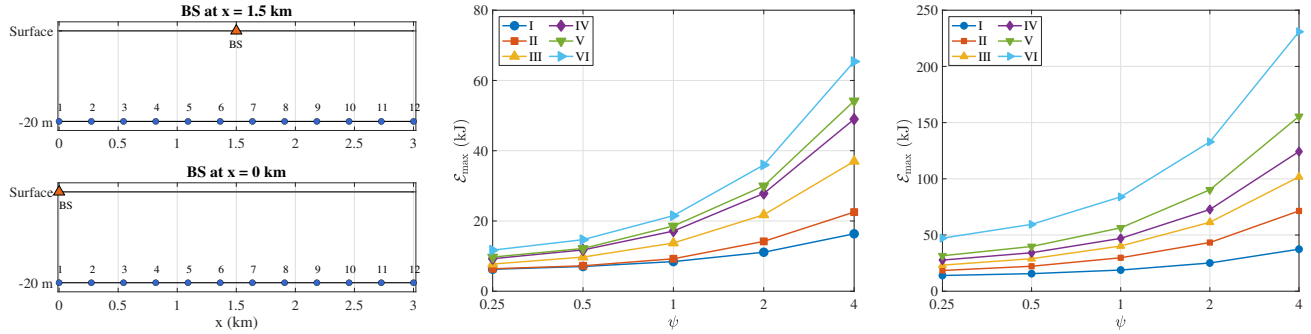

(a) (b) (c)

Fig. 1: (a) UWSN topology with 12 nodes and two BS positions. (b) $\mathcal{E}_{\max}$ (kJ) vs. ψ for BS at $x = 1.5$ and (c) at $x = 0$ km.

corresponding positive flow (i.e., $u_{ij}^{kl} \geq 1$), thus maintaining consistency between flow allocation and path selection.

$$\begin{aligned} u_{ij}^{kl} &\leq Q_k \mathcal{N}_\tau n_{ij}^{kl}, \\ n_{ij}^{kl} &\leq u_{ij}^{kl}, \end{aligned} \qquad \forall (i,j) \in \mathcal{A},\ k \in \mathcal{W}, l \in \mathcal{L}. \tag{6}$$

Constraint (7) imposes that for each source node-k, any path-l originates from at most one outgoing link of node-i, and that each link (i,j) is assigned to at most one path index for the same source node, thus preventing multiple path overlaps.

$$\begin{aligned} &\sum_{(i,j)\in\mathcal{A}} n_{ij}^{kl} \leq 1, \quad \forall i \in \mathcal{W},\ k \in \mathcal{W},\ l \in \mathcal{L} \\ &\sum_{l=1}^{\eta_l} n_{ij}^{kl} \leq 1, \quad \forall (i,j) \in \mathcal{A},\ k \in \mathcal{W} \end{aligned} \tag{7}$$

Constraint (8) guarantees, for ordering purposes, that the number of packets transmitted by source node-k on routing path-l decreases as the path index l increases.

$$\sum_{(j,1)\in\mathcal{A}} u_{j1}^{k(l+1)} \leq \sum_{(j,1)\in\mathcal{A}} u_{j1}^{kl},\ \forall k \in \mathcal{W},\ l \in \mathcal{L} \tag{8}$$

Constraint (9) prevents the occurrence of phantom flows by activating the flow variable u_{ij}^{kl} if $n_{ij}^{kl} = 1$. The big-M parameter relaxes these constraints when $n_{ij}^{kl} = 0$, forcing u_{ij}^{kl} to match z_k^l only if the associated link is used [10]. In this constraint, we choose $M = 1 \times 10^4$.

$$\begin{aligned} u_{ij}^{kl} - M(1 - n_{ij}^{kl}) &\leq z_k^l, \\ u_{ij}^{kl} + M(1 - n_{ij}^{kl}) &\geq z_k^l, \end{aligned} \qquad \forall (i,j) \in \mathcal{A},\ k \in \mathcal{W},\ l \in \mathcal{L} \tag{9}$$

Constraint (10) defines the control packet flow on link-(i,j) (i.e., w_{ij}^{kl}) with respect to the control packet frequency ψ.

$$w_{ij}^{kl} = \psi \mathcal{N}_\tau (n_{ij}^{kl} + n_{ji}^{kl}), \quad \forall (i,j) \in \mathcal{A},\ k \in \mathcal{W},\ l \in \mathcal{L} \tag{10}$$

Constraint (11) enforces the *non-uniform k-connectivity* requirement by ensuring that each source node-k maintains at least κ_n distinct paths to the BS, where the connectivity level κ_n varies across source groups $n \in S_P$. Here, S_P is the index set of distinct subsets of nodes and $\mathcal{W}_n$ denotes the n-th subset of sensor nodes, each assigned a k-connectivity value κ_n, with $\mathcal{W} = \bigcup_{n\in S_P} \mathcal{W}_n$ and $\mathcal{W}_n \cap \mathcal{W}_m = \emptyset$ for $n \neq m$.

$$\sum_{(k,j)\in\mathcal{A}} \sum_{l=1}^{\eta_l} n_{kJ}^{kl} \geq \kappa_n, \quad \forall k \in \mathcal{W}_n,\ n \in S_P \tag{11}$$

Constraint (12) ensures that paths from a source node-k are node-disjoint, with each relay node used in at most one path. With (11), this constraint guarantees link-disjointness.

$$\sum_{(i,j)\in\mathcal{A}} \sum_{l=1}^{\eta_l} n_{ij}^{kl} \leq 1, \ \sum_{(j,i)\in\mathcal{A}} \sum_{l=1}^{\eta_l} n_{ji}^{kl} \leq 1, \quad \forall\, i \in \mathcal{W} \backslash k, k \in \mathcal{W} \tag{12}$$

Constraint (13) limits each node's total transmission and reception cost for both data and control packets.

$$\begin{aligned} &\sum_{l=1}^{\eta_l} \sum_{k\in\mathcal{W}} \Bigg[\sum_{(i,j)\in\mathcal{A}} \mathcal{E}_{\mathrm{T},ij}^{*} (u_{ij}^{kl} L_{\mathrm{pkt}} + w_{ij}^{kl} L_{\mathrm{cnt}}) \\ &+ \sum_{(j,i)\in\mathcal{A}} \mathcal{E}_{\mathrm{R}} (u_{ji}^{kl} L_{\mathrm{pkt}} + w_{ji}^{kl} L_{\mathrm{cnt}}) \Bigg] \leq \mathcal{E}_{\max}, \quad \forall i \in \mathcal{W} \end{aligned} \tag{13}$$

Constraint (14) guarantees that the total time a node spends transmitting, receiving, or remaining inactive due to interference from nearby links does not exceed its available bandwidth. The interference parameter χ_{jm}^{i} equals 1 if node-i lies within the interference range of link (j,m), and 0 otherwise.

$$\begin{aligned} &\sum_{k\in\mathcal{W}} \sum_{l=1}^{\eta_l} \Bigg[\sum_{(i,j)\in\mathcal{A}} \left(u_{ij}^{kl} \frac{L_{\mathrm{pkt}}}{\lambda_{\mathrm{data}}} + w_{ij}^{kl} \frac{L_{\mathrm{cnt}}}{\lambda_{\mathrm{data}}} \right) \\ &+ \sum_{(j,i)\in\mathcal{A}} \left(u_{ji}^{kl} \frac{L_{\mathrm{pkt}}}{\lambda_{\mathrm{data}}} + w_{ji}^{kl} \frac{L_{\mathrm{cnt}}}{\lambda_{\mathrm{data}}} \right) \\ &+ \sum_{(j,m)\in\mathcal{A}\backslash\{i\}} \left(u_{jm}^{kl} \chi_{jm}^{i} \frac{L_{\mathrm{pkt}}}{\lambda_{\mathrm{data}}} + w_{jm}^{kl} \chi_{jm}^{i} \frac{L_{\mathrm{cnt}}}{\lambda_{\mathrm{data}}} \right) \Bigg] \\ &\leq \mathcal{N}_\tau \times \tau, \quad \forall i \in \mathcal{V} \end{aligned} \tag{14}$$

Constraint (15) specifies the bounds of the decision variables, enforcing non-negativity for flow and data injection variables

and binary values for path selection variables.

$$u_{ij}^{kl}, w_{ij}^{kl} \geq 0, n_{ij}^{kl} \in \{0,1\},\ \forall (i,j) \in \mathcal{A},\ k \in \mathcal{W},\ l \in \mathcal{L}$$
$$z_k^l \geq 0, \forall k \in \mathcal{W},\ l \in \mathcal{L} \tag{15}$$

III. Analysis

This section presents the optimal MILP solutions for a wide range of k-connectivity configurations. The MILP model is implemented in Python and solved with GUROBI [11].

TABLE II: Uniform and non-uniform k-connectivity configurations. $\mathcal{W}_1$, $\mathcal{W}_2$, and $\mathcal{W}_3$ require $\kappa_1 = 1$, $\kappa_2 = 2$, and $\kappa_3 = 3$, with $\mathcal{W}$ their union (I, III, VI: *uniform*; II, IV, V: *non-uniform*).

Config.	Node groups	$\mathcal{W}$
I	$\mathcal{W}_1 = \{1, 2, \ldots, 12\}$	$\mathcal{W}_1$
II	$\mathcal{W}_1 = \{1, 3, 4, 10, 11, 12\}$ $\mathcal{W}_2 = \{2, 5, 6, 7, 8, 9\}$	$\mathcal{W}_1 \cup \mathcal{W}_2$
III	$\mathcal{W}_2 = \{1, 2, \ldots, 12\}$	$\mathcal{W}_2$
IV	$\mathcal{W}_1 = \{4, 5, 6, 8\}$ $\mathcal{W}_2 = \{1, 2, 10, 11\}$ $\mathcal{W}_3 = \{3, 7, 9, 12\}$	$\mathcal{W}_1 \cup \mathcal{W}_2 \cup \mathcal{W}_3$
V	$\mathcal{W}_2 = \{2, 4, 7, 9, 10, 12\}$ $\mathcal{W}_3 = \{1, 3, 5, 6, 8, 11\}$	$\mathcal{W}_2 \cup \mathcal{W}_3$
VI	$\mathcal{W}_3 = \{1, 2, \ldots, 12\}$	$\mathcal{W}_3$

Table II summarizes the six k-connectivity configurations considered in this study. In each configuration, sensor nodes are assigned to different groups $\mathcal{W}_1$, $\mathcal{W}_2$, and $\mathcal{W}_3$, which require connectivity levels of $\kappa_1 = 1$, $\kappa_2 = 2$, and $\kappa_3 = 3$, respectively. The *uniform k-connectivity* cases (Configs. I, III, and VI) correspond to classical k-connected networks, where all nodes have the same requirement: Config. I represents a 1-connected network ($\kappa_1 = 1$), Config. III a 2-connected network ($\kappa_2 = 2$), and Config. VI a 3-connected network ($\kappa_3 = 3$). In contrast, the *non-uniform k-connectivity* cases (Configs. II, IV, and V) reflect heterogeneous reliability requirements by mixing different groups of nodes. For example, in Config. IV, nodes 4, 5, 6, and 8 are 1-connected to the BS, nodes 1, 2, 10, and 11 are 2-connected, and nodes 3, 7, 9, and 12 are 3-connected. Sensor nodes are assumed to be grouped randomly; however, for analysis, certain nodes may be considered more critical as their failure would disproportionately affect coverage or connectivity.

Figs. 1b and 1c show the optimal $\mathcal{E}_{\max}$ values (in kJ) obtained from the MILP model for BS deployments at $x = 1.5$ km and at $x = 0$ km, respectively. We choose five ψ values (i.e., $\psi = \{0.25, 0.5, 1, 2, 4\}$) to investigate the impact of control packet frequency of the results.

Uniform k-connectivity configurations highlight the baseline impact on energy consumption: Configs. I, III, and VI yield $\mathcal{E}_{\max}$ values up to 37.38 kJ, 101.74 kJ, and 230.81 kJ, respectively, corresponding to up to 2.72-fold and 6.17-fold increases over the 1-connected case. The *non-uniform k-connectivity* cases show that partial enforcement of higher-k requirements leads to lower energy consumption than the fully 3-connected uniform case, yet still entails significant overhead compared to the 1-connected case. Config. II (mix of 1- and 2-connected nodes) raises $\mathcal{E}_{\max}$ values by up to 1.91 times relative to Config. I, Config. IV (mix of 1-, 2-, and 3-connected nodes) by up to 3.32 times, and Config. V (mix of 2- and 3-connected nodes) by up to 4.16 times.

Across all configurations, increasing ψ from 0.25 to 4 raises $\mathcal{E}_{\max}$ by about 2.62 to 5.59 times. This reflects the high energy demand required to sustain multiple paths under higher control packet frequency. By contrast, the impact of BS deployment is more limited than that of ψ and connectivity. For example, $\mathcal{E}_{\max}$ at $x = 0$ km is between 2.22 and 4.05 times higher than at $x = 1.5$ km. Thus, placing the BS nearer the network center reduces energy consumption, but its effect is minor compared to the sharp growth from higher connectivity.

IV. Conclusion

This study examines the trade-off between reliability and energy efficiency in UWSNs for coastal applications. We propose a *non-uniform k-connectivity* model using a MILP framework that incorporates energy costs in underwater acoustic channels and link maintenance costs. Our results show that *non-uniform k-connectivity* offers a better reliability–energy efficiency balance, reducing the energy overhead to 4.16-fold instead of 6.17-fold for a fully 3-connected network, while higher control packet frequency amplifies energy demand by up to 5.59-fold and BS deployment has only a moderate effect, increasing the energy consumption by up to 4.05 times. Future work will focus on improving scalability through MILP decomposition and relaxation techniques for large-scale networks.

References

[1] T. Qiu, Z. Zhao, T. Zhang, C. Chen, and C. L. P. Chen, "Underwater internet of things in smart ocean: System architecture and open issues," *IEEE Trans. Ind. Informat.*, vol. 16, no. 7, pp. 4297–4307, Jul. 2020.

[2] X. Wei, H. Guo, X. Wang, X. Wang, and M. Qiu, "Reliable data collection techniques in underwater wireless sensor networks: A survey," *IEEE Commun. Surv. Tuts.*, vol. 24, no. 1, pp. 404–431, 2022.

[3] H. U. Yildiz, V. C. Gungor, and B. Tavli, "Packet size optimization for lifetime maximization in underwater acoustic sensor networks," *IEEE Trans. Ind. Informat.*, vol. 15, no. 2, pp. 719–729, Feb. 2019.

[4] Z. A. Dagdeviren, V. K. Akram, O. Dagdeviren, B. Tavli, and H. Yanikomeroglu, "k-connectivity in wireless sensor networks: Overview and future research directions," *IEEE Netw.*, vol. 37, no. 3, pp. 140–145, May/Jun. 2023.

[5] M. Cobanlar, V. K. Akram, O. Dagdeviren, and B. Tavli, "Analysis of the tradeoff between network lifetime and k-connectivity in WSNs," in *Proc. Telecommun. Forum (TELFOR)*, 2018, pp. 1–4.

[6] M. Cobanlar, H. U. Yildiz, V. K. Akram, O. Dagdeviren, and B. Tavli, "On the tradeoff between network lifetime and k-connectivity based reliability in UWSNs," *IEEE Internet Things J.*, vol. 9, no. 23, pp. 24 444–24 452, Dec. 2022.

[7] M. A. Khan, N. Javaid, A. Majid, M. Imran, and M. Alnuem, "Dual sink efficient balanced energy technique for underwater acoustic sensor networks," in *Proc. Int. Conf. Adv. Inform. Netw. Appl. Work. (WAINA)*, 2016, pp. 551–556.

[8] H. Xu, F. Ye, H. Su, and C. Su, "Energy-efficient relay selection and power allocation optimization for lifetime maximization in underwater acoustic sensor networks," *IEEE Sens. J.*, pp. 1–1, 2025.

[9] J. Zhu, K.-L. Hung, and B. Bensaou, "Tradeoff between network lifetime and fair rate allocation in wireless sensor networks with multi-path routing," in *Proc. ACM Int. Symp. Model. Anal. Simul. Wirel. Mobile Syst. (MSWiM)*, 2006, pp. 301–308.

[10] T. Bektas and L. Gouvei, "Requiem for the Miller–Tucker–Zemlin subtour elimination constraints?" *Eur. J. Oper. Res.*, vol. 236, no. 3, pp. 820–832, Aug. 2014.

[11] Gurobi Optimization, LLC, *Gurobi Optimizer Reference Manual*, 2025. [Online]. Available: https://www.gurobi.com